doi: 10.1111/j.1365-3121.2007.00788.x

Relative fracture velocities based on fundamental characteristics of joint-surface morphology

Ram Weinberger[1] and Dov Bahat[2]

[1]*Geological Survey of Israel, 30 Malkhei Israel St., Jerusalem 95501, Israel;* [2]*Department of Geological and Environmental Sciences, Ben Gurion University of the Negev; and the Deichmann Rock Mechanics Laboratory of the Negev, Beer Sheva 84105, Israel*

ABSTRACT

Two different joint surface morphologies, plumes and rib marks, characterize joint surfaces, but the mechanical conditions that lead to the formation of either of the morphologies are not understood well. We studied two orthogonal joint sets that cut the same Santonian chalk beds in the Judea Desert, Israel. Joints of the J_1 set are systematic, relatively long, characterized by almost exclusively by plumes and predate the shorter, non-systematic joints of the J_2 set that are characterized by rib marks. Joints of the J_1 set formed at high stress during deformation of the Syrian Arc folding in the Late Senonian. Joints of the J_2 set formed at lower stress that occurred because of stress relaxation after the formation of the J_1 joints. A mechanical analysis indicates that the J_1 joints propagated at subcritical velocities several orders of magnitude faster than the J_2 joints. Based on previously published data of laboratory tests, the plumes and the rib marks are semi-quantitatively placed on the subcritical part of the fracture velocity vs. stress-intensity factor diagram.

Terra Nova, 20, 68–73, 2008

Introduction

The brittle upper crust contains a variety of structures, the most common of which are joints. They profoundly control the physiography of many spectacular landforms and play an important role in the transport of fluids such as water, magma and hydrocarbons (e.g. Pollard and Aydin, 1988). Establishment of reliable relationships between joints and their cause provides important tools for inferring the loading conditions and mechanical behaviour of rocks not only in the field of structural geology but also in such fields as volcanology, palaeoseismology and engineering geology. For example, the propagation rate of the preceding joints affects the emplacement of magmatic intrusions (Rubin, 1995; Weinberger *et al*., 2000) and controls the fracture mechanics of earthquake-induced clastic dikes (Levi *et al*., 2006).

Joints, particularly those that are not filled, have a distinctive surface morphology. The analysis of joint-surface morphology known as fractography is a useful tool in deciphering the palaeo-fracture conditions, helping to identify the mechanical and tectonic processes that produced fracturing. Two different surface morphologies, plumes and rib marks ornament the parent joint surfaces (Fig. 1). The plumes consist of trains of barbs that form feather-like morphologies that fan away from the joint-origin point and the plume axis towards the peripheries of the joint plane. The rib marks consist of ridges of conchoidal appearance that concentrically propagate from the joint-origin point. Transitional markings show that superposition of plumes and rib marks are common and that rib marks and plumes form at right angle to each other. Joint-surface morphologies have been used for decades for inferring joint nucleation, propagation and termination (e.g. Woodworth, 1896; De Freminville, 1914; Hodgson, 1961; Bankwitz, 1966; Bahat, 1979; Kulander *et al*., 1979; Helgeson and Aydin, 1991; Weinberger, 1999). They develop largely because of local twists and tilts during propagation (Lawn, 1993), but the mechanical conditions that lead to the formation of either of the morphologies are still not understood well.

Previous investigations have shown preferential distribution of joint-surface markings in host lithologies, selected joint sets and fracture provinces. In the Appalachian Plateau province, certain joint sets favoured certain lithologies, such as joints striking east north-eastward, which are common in shales but less developed in siltstone (Sheldon, 1912). In the same fracture province, plumes are rare on fold-axis parallel joints in shales, but commonly occur on fold-axis perpendicular joints dissecting siltstones (Parker, 1942; Bahat and Engelder, 1984). The studies made indicate that the mechanical properties of the host rock are important variables in influencing the development of regional joint sets as well as their surface morphology. In the Beer Sheva syncline, Israel, joints in the Lower Eocene chalks display coarse plumes as well as rib marks on both fold-axis parallel and fold-axis perpendicular joints. In contrast, joints in the Middle Eocene chalks of the same syncline exhibit delicate plumes and rarely show rib marks (Bahat, 1991), exemplifying the influence of different tectonic conditions on the rock fractography when occurring in the same rock type.

Quantitative fractography has recently taken the lead in joint investigation by harnessing two tools; fracture mechanics and experimental results from material sciences (e.g. Cooke and Pollard, 1996). A key parameter in characterizing the fracture mechanics properties of a fracture is its velocity (Wiederhorn, 1967). Fractography has shown that fracture velocity of joints may vary, not only from slow propagation to a rapid one, but also in cycles (Bahat *et al*., 2005, p. 362). Thus, fracture velocity estimation provides an important record

Correspondence: Dr Ram Weinberger, Division of Engineering Geology and Geological Hazards, Geological Survey of Israel, 30 Malkhe Israel St., Jerusalem 95501, Israel. Tel.: +972 2 531 4273; fax: +972 2 538 0688; e-mail: rami@geos.gsi.gov.il

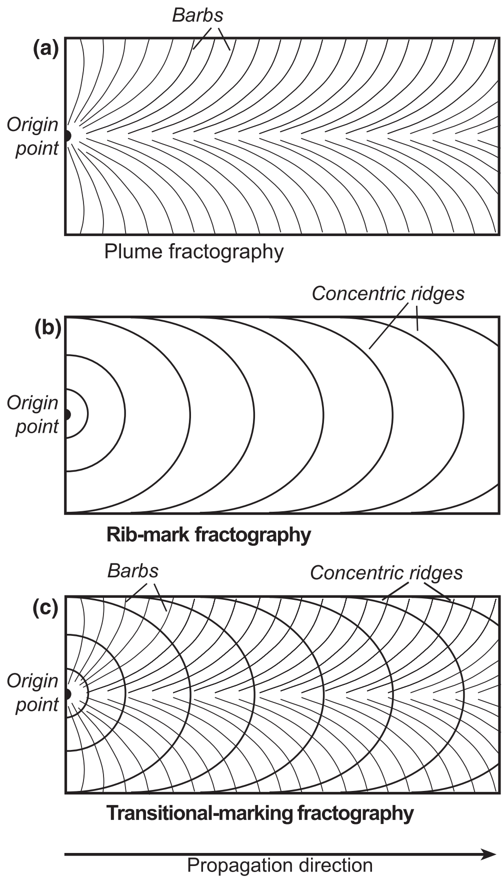

Fig. 1 Fracture markings on joint surfaces: (a) plume; (b) rib marks; (c) transitional markings of both plume and rib marks.

of fracture history and insight into the fracture mechanism.

In analysing joint velocity, one needs to take into account the local geological conditions that influence the jointing process, such as layer thickness, joint genetics, pore pressure, lithology and fracture province. In this study, we eliminate the role played by these influences by examining fractographies that occur in a series of adjacent outcrops within a single fracture province and structural position. A comparison between plumes and rib marks is made on joints cutting the same Santonian chalks in the Judea Desert, Israel, which enables us to elucidate the relative fracture velocities and the tectono-mechanical conditions that lead to the formation of either plumes or rib marks.

Geologic setting

The joints studied cut the Santonian Menuha Formation, which overlies the Cretaceous Judea Group at the western margin of the Dead Sea Transform (Fig. 2). The Menuha Formation consists mainly of chalk and is subdivided into two members (Honigstein, 1984; Mor, 1987). We focus on joints that cut the massive, whitish chalk of the lower member. All outcrops in this study are located 20–40 m above the top of the Judea Group (top Turonian). The beds studied dip westward less than 5^{o} and are part of an open fold (Judea Desert syncline, Fig. 2) that strikes north-eastward. This fold is part of the sigmoid fold bundle known as the 'Syrian Arc folding system' (Krenkel, 1924), which crosses the Levant. The Syrian Arc folds have many common geological characteristics, including north north-eastward trends (in Israel), asymmetry because of the presence of deep-seated reverse faults, and a multiphase history of deformation. Ages of folding range from Turonian to Neogene, with peaks of deformation rate discerned in the Late Turonian, Late Senonian, post Middle Eocene and possibly late Quaternary (Flexer, 2001, and references therein).

Prominence of two joint sets

In the Judea Desert, there are two well-developed joint sets striking north-westward (316°, the J_1 set) and north-eastward (050°, the J_2 set), which have quasi-orthogonal directions (Fig. 3). The J_1 set is almost perpendicular to the trend of the Judea Desert syncline, whereas the J_2 set is sub-parallel to its trend. The outcrops studied are located in Wadi Darga and arranged along two perpendicular traverses; one is sub-parallel to the J_1 set and the other, to the J_2 set. This arrangement enables an excellent view of the joint-surface morphologies along fresh road cuts in which both joint sets are found within the same chalk beds and are bounded between the same mechanical boundaries. Crosscutting relations show unequivocally that the systematic joints of the J_1 set always predated the non-systematic joints of the J_2 set, producing a 'ladder-like' structure (e.g. Rawnsley *et al.*, 1998; Bai *et al.*, 2002; Fig. 4). This order is supported by close-up fractographic observations that show either J_2 joints terminating at J_1 joints, J_2 joints initiating at J_1 joints, or, rarely, J_2 joints cutting J_1 joints (Figs 4 and 5).

Two joint-surface morphologies, plumes (Fig. 5) and rib marks (Fig. 6), are of particular concern in this study. The plumes extend horizontally and are sometimes longer than 3 m on vertical joints. They occur almost exclusively on the J_1 joints. Occasionally, joints bearing plumes are associated with en-echelon fringes. Radial plumes are occasionally superposed on the rib marks, forming transitional markings. This morphology distinguishes the relatively short (< 0.5 m) J_2 joints that are bounded between adjacent, closely spaced J_1 joints. The two joint-surface morphologies are distinctly associated with a particular joint set. Almost all the J_2 joints are characterized by rib marks, and 85% of the J_1 joints are solely marked by plumes; the other 15% of the J_1 joints by transitional markings.

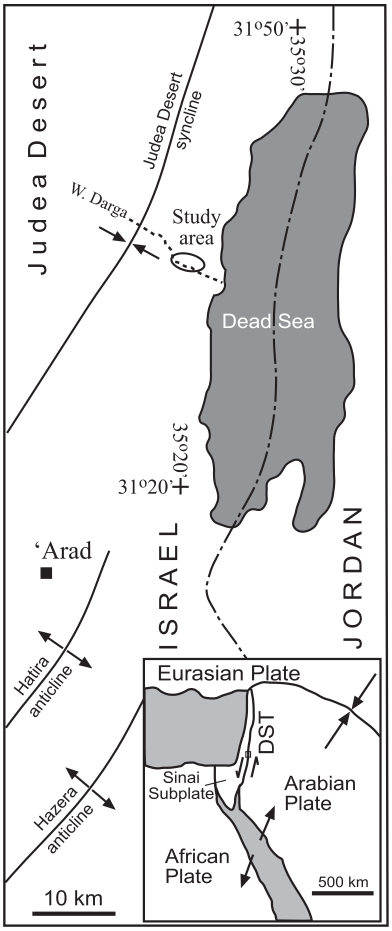

Fig. 2 Local setting of the study area, including nearby large NE-trending folds related to the Syrian Arc system. Arrows indicate dip directions of fold limbs in Judea Desert. Inset: A regional setting of the study area (marked by a rectangle). Arrows indicate plate divergence along the Red Sea, plate convergence along the Zagros, and a sinistral movement along the Dead Sea Transform (DST).

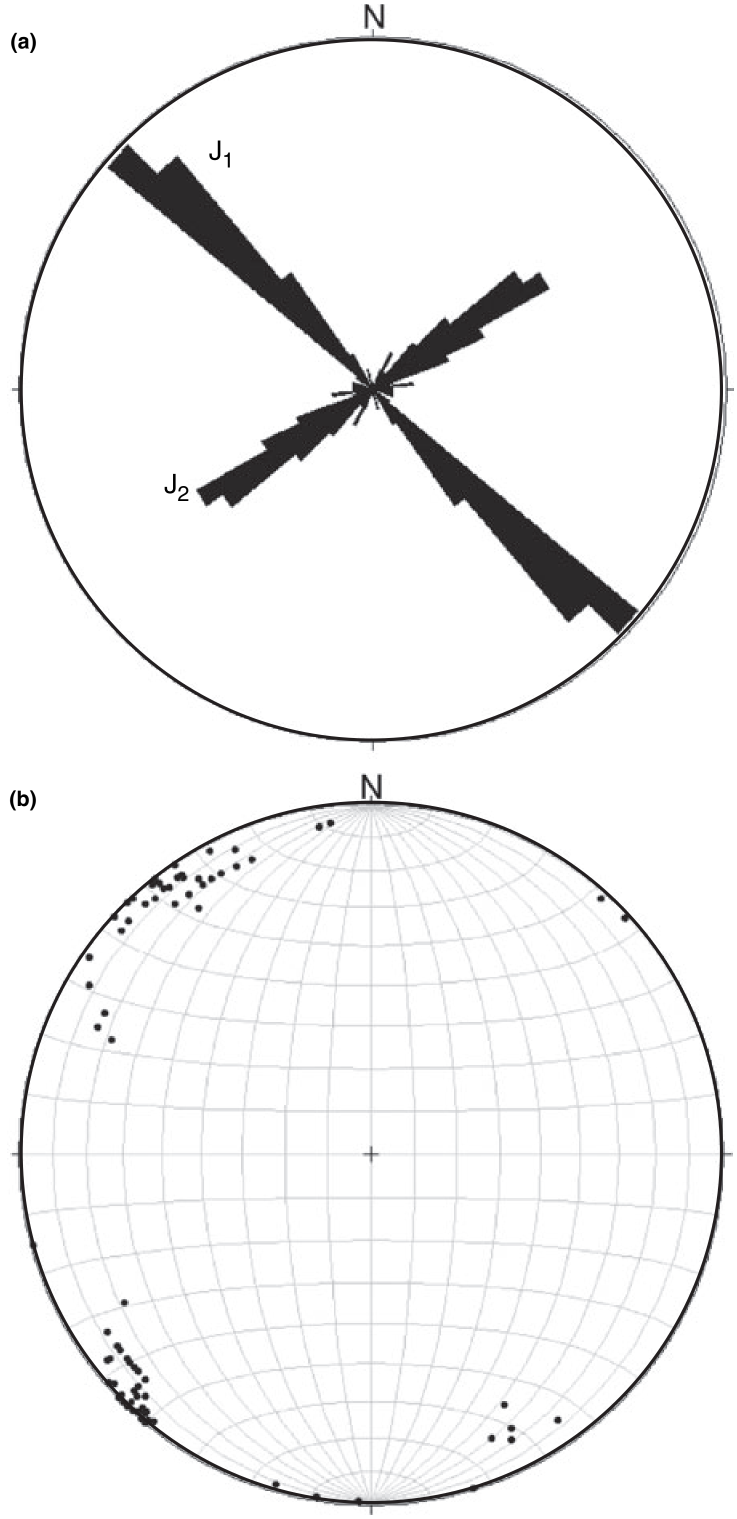

Fig. 3 Diagrammatic summaries of measured fracture parameters from the lower member of the Santonian Menuha Formation in the Judea Desert. (a) Rose diagram of joint strikes showing two sets, J_1 (316°) and J_2 (050°). Sector length is proportional to number of joints ($N = 91$); (b) lower hemisphere equal area stereographic projection of poles to fracture planes. The 95% confidence interval of joint set J_1 and J_2 is $a_{95} = 7^o$ and $a_{95} = 15^o$, respectively.

Interpretation of field observations

We documented the consistency of joint orientations, crosscutting relations, and preferential distribution of surface morphology within the same chalk beds and structural position. Hence, grain size, flaw distribution and durability of the host rock, which play a major role in fracturing sedimentary beds elsewhere (e.g. Weinberger, 2001), did not play a role in the present case study. This suggests that the formation of preferential joint-surface markings is related to different

Fig. 4 Systematic joints of the J_1 set and non-systematic joints of the J_2 set forming a ladder-like structure. Outcrop height is about 6 m.

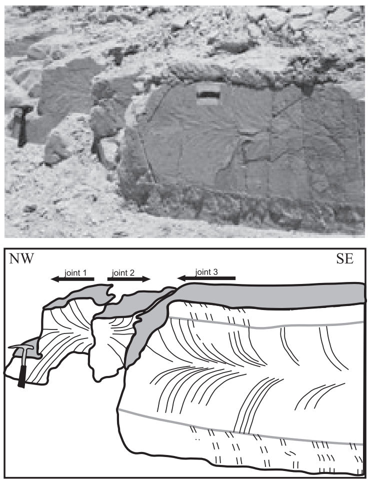

Fig. 5 Three systematic joints of the J_1 set marked by plumes. Note propagation in opposite directions of adjacent joints, and the formation of systematic en-echelon cracks at the fringes of joint 3. The en-echelon cracks were considerably affected by erosion and, hence, are drawn only schematically. Traces of joints from the J_2 set are seen along the surface of joint 3 (see on the photo only).

loading conditions at the times of J_1 and J_2 jointing.

We interpret the field observations along three lines of arguments below: First, we interpret the tectonic conditions under which sets J_1 and J_2 were formed. Second, we assemble experimental results, which enable correlating the joint-surface morphologies of the two sets with their mechanical fracture conditions and expected fracture velocities. Finally, we apply fracture mechanics rules in calculating the relative fracture velocities of the propagating joints.

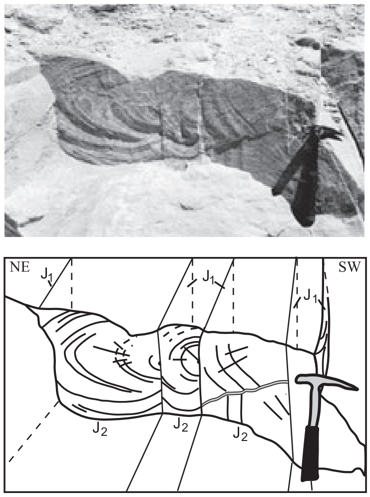

Fig. 6 Photograph and drawing showing the surface morphologies of J_2 joints and crosscutting relations between the J_1 and J_2 joints. The inferred initiation points (black dots) of the J_2 joints are located along the surface of the J_1 joints and their rib marks end abruptly against adjacent J_1 joints, indicating that the J_1 joints formed before the J_2 joints. Dashed lines mark the hidden traces of the J_1 joints that are ornamented by plumes.

The first deformation stage of the Syrian Arc folding was in the Late Turonian (Bentor *et al.*, 1970) predating the deposition of the Menuha chalk beds. Joint sets J_1 and J_2 must have formed during the Senonian, most likely associated with the intense deformation in the Late Campanian (Steinitz, 1974; Bahat, 1991, p. 262). A later deformation stage of the Syrian Arc in the Eocene formed joints (Bahat, 1991, p. 241) that differ in their orientations from those recorded in the J_1 and J_2 sets. We follow the model of stress relaxation by Price (1966) and others (e.g. Hancock *et al.*, 1987; Rives *et al.*, 1994) and suggest that stress relaxation and a switch in the direction of the maximum tension took place between the early formation of the J_1 joints, and the later formation of the J_2 joints. Based on the above mechanism, the J_2 joints grew under lower stresses than the J_1 joints (see below).

On the basis of extended observations (Bahat *et al.*, 2005, p. 128) we set a few criteria for distinguishing rib marks that form rapidly (hereafter, *undulations*) from rib marks which are associated with post arrest or slow crack propagation (hereafter, *arrest marks*). Undulations are sinusoidal in profiles, smooth on their crests, separated from each other, and maintain parallelism between successive ones. On the other hand, arrest marks often show more complex fractographies; they strongly deviate from symmetric curving profiles, their crests are often sharp and occasionally they deviate from parallelism between successive marks. All the above criteria of arrest marks are recognized on the surfaces of the J_2 joints (Fig. 6), but not on the surfaces of the J_1 joints, which, up to their final termination, did not arrest.

Murgatroyd (1942) suggested that an arrest mark 'is actually a high point where a fracture which had been moving upward before coming to rest resumed its course in a downward direction when it recommenced'. More recently, fracture experimentation on soda-lime glass (Yoda, 1990) demonstrated that arrest marks were produced by repeatedly unloading the specimen, showing the crack front during crack growth. Michalske (1977), Wiederhorn *et al.* (2002) and Guin and Wiederhorn (2003) investigated fractures in soda-lime glass microscopic slides and found that arrest marks appeared only on resuming fracture propagation after a hold period of the glass below the crack-growth threshold. Hence, some of these experiments show that the arrest marks develop on resuming propagation after arrest, while other results point to slow crack velocities during crack propagation. Accordingly, it seems legitimate to hypothesize that arrest marks propagate between two end-member velocities: one is associated with 'post-arresting' arrest marks that start from stand still and the other with 'readjusting' arrest marks (Murgatroyd, 1942) at slow velocities.

Kerkhof (1975) observed that arrest marks were induced in plate glass at fracture velocity below $V = 4 \times 10^{-5}$ m s^{-1} and stress-intensity factor $K_I < 0.73$ MPa m$^{1/2}$ that correspond to the range of regions I and II in the V vs. K diagram (Fig. 7). Accordingly, we propose that surface markings in rocks that display arrest marks reflect the range of regions I and II. Plumes (striae) developed on a smooth fracture surface of soda-lime

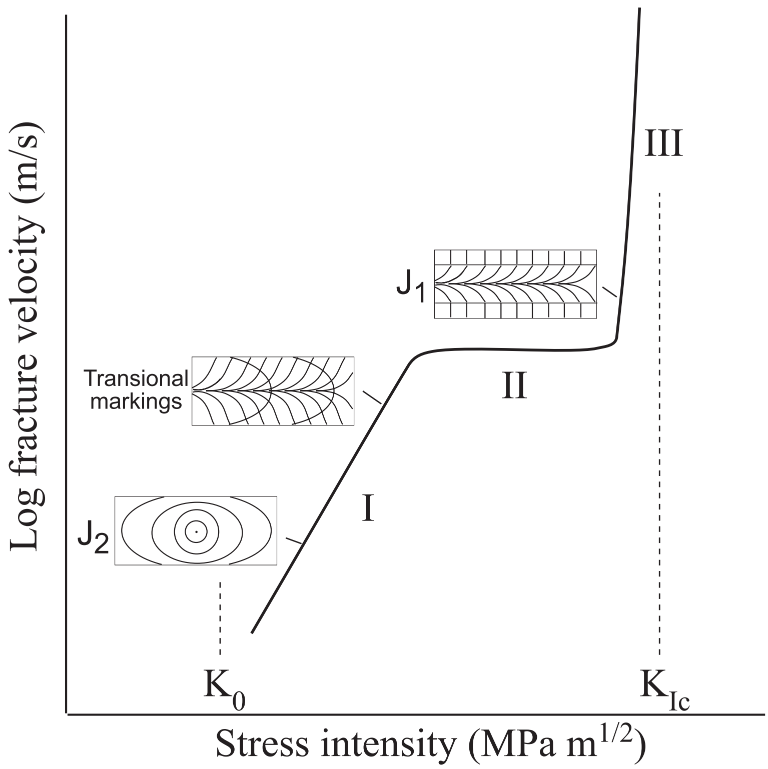

Fig. 7 Schematic drawing of (log) fracture velocity vs. stress-intensity factor behaviour of subcritical growth of tensile cracks (after Atkinson and Meredith, 1987). K_{Ic} is the fracture toughness and K_0 is the stress corrosion limit. Joint-surface morphologies are arranged based on the interpretation of the Menuha chalk fractography. Plumes with en-echelon fringes ornamenting the J_1 set evolved during relatively fast fracture velocity (Region III); rib marks ornamenting the J_2 set evolved during relatively slow fracture velocity (Region I); and transitional markings evolved during intermediate fracture velocity (Regions I–II).

silica glass in water when the velocity of fracture propagation reached about 10^{-2} m s^{-1} at around K_I = 0.7–0.8 MPa m$^{1/2}$ (Michalske, 1984; Fig. 1). This was above the mid range between the stress corrosion limit, K_I = 0.3 MPa m$^{1/2}$, and the fracture toughness K_{Ic} = 0.9 ± 0.1, i.e. these plumes formed in the range of regions II to III. Thus, plumes form at higher fracture velocities and stress intensities than arrest marks. The occurrence of arrest marks superposed by radial plumes on joint surfaces suggests that occasionally plumes may form under fracture conditions similar to those that produce arrest marks. Possibly, this superposition occurs at the upper velocity ranges of arrest marks and lower velocity ranges of plumes.

The above observations and laboratory experiments led us to analyse semi-quantitatively the fracture velocities of the J_1 and J_2 joints and to locate the plumes and the arrest marks on the *V* vs. *K* diagram (Fig. 7) as follows. For a first-order approximation, we assume that extension exists only perpendicular to J_1 joints and consider the horizontal stresses. Tension is defined as positive and all stress components should be regarded as effective stresses. We define the joint-normal maximum tension σ_1 and the joint-parallel minimum tension σ_2. In such cases, the in-plane stress ratio σ_1/σ_2 is proportional to $(1 - \nu)/\nu$ (Jaeger and Cook, 1979, p. 113), where ν is the Poisson's ratio of the chalk beds. For a typical value of $\nu = 0.2$ for chalk $\sigma_1/\sigma_2 = 4$, indicating that at the time of the J_1 jointing and before the formation of the J_2 joints, the stress is four times higher (more tensional) perpendicular to the J_1 joints than parallel to the J_1 joints (e.g. perpendicular to the J_2 joints). Ignoring the effect of joint interaction, the stress-intensity ratio is $K_{I(1)}/K_{I(2)} \propto \sigma_1(\pi \cdot l_1)^{1/2}/\sigma_2(\pi \cdot l_2)^{1/2} \approx 4$, where $K_{I(1)}$ and $K_{I(2)}$ are the stress-intensity factors of the J_1 and J_2 joints at arbitrary equal lengths l_1 and l_2, respectively. Because in the subcritical regime the fracture velocity $V \propto K_I^n$, where *n* is a constant that depends on the mechanism responsible for fracture growth (Atkinson and Meredith, 1987), the fracture velocity of the J_1 joints V_1 could be 4^n faster than the fracture velocity of the J_2 joints V_2. The J_1 joints show more lateral propagation than do the J_2 joints, indicating that this factor (4^n) should be regarded as a minimum value. Atkinson and Meredith (1987) indicated that for diffusion-controlled fracture growth *n* is often in the range of 2–10, whereas for stress-corrosion fracture growth *n* may be in the range of 20–50. Hence, even for lower values of *n*, V_1 was several orders of magnitude faster than V_2. Furthermore, based on previous studies (e.g. Bahat, 1991, p. 234; Bahat *et al.*, 2003), we can hypothesize that the J_1 joints characterized by plumes propagated at V_1 between 10^{-2} and 10^{-4} m s^{-1} and, concomitantly, the J_2 joints characterized by rib marks propagated at V_2 between 10^{-4} and 10^{-7} m s^{-1} (Michalske, 1984; Bahat *et al.*, 2005, p. 359) in agreement with the above laboratory data. Noticeably, the relative location of the two fundamental joint-surface morphologies and the transitional one on the *V* vs. *K* diagram is based on the present analysis of field observations. However, the division into the different subcritical regimes follows previous studies in glass (e.g. Wiederhorn and Bolz, 1970) and granite (Bahat *et al.*, 2003).

Conclusions

Joints cutting the Santonian chalk beds in the Judea Desert and displaying plumes propagated at subcritical velocities 2–3 orders of magnitude greater and at higher stress-intensity conditions than joints displaying arrest marks in the same beds. This fractographic interpretation is corroborated by the observation that the J_1 joints are systematic and long whereas the J_2 joints are non-systematic and short. This relationship is also consistent with the J_1 jointing during the intense folding of the Syrian Arc in the Late Senonian.

Acknowledgements

This study was supported by a grant from the Israeli Ministry of National Infrastructures, Earth Sciences Administration. We thank Ze'ev B. Begin, Vladimir Lyakhovsky and Tsafrir Levi for fruitful discussions, Michele Cooke for comments and suggestions on an early version of the paper, and Aya Manor and Yoav Borenstein for their assistance in the field and office.

References

Atkinson, B.K. and Meredith, P.G., 1987. The theory of subcritical crack growth with implications to minerals and rocks. In: *Fracture Mechanics of Rock* (B.K. Atkinson, ed.), pp. 111–166. Academic Press, London.

Bahat, D., 1979. Theoretical considerations on mechanical parameters of joint surfaces based on Atkinson, B.K., and Meredith, P.G., 1987. The theory of subcritical crack growth with studies on ceramics. *Geol. Mag.*, **11**, 81–92.

Bahat, D., 1991. *Tectonofractography*. Springer-Verlag, Heidelberg, 354 pp.

Bahat, D. and Engelder, T., 1984. Surface morphology on cross-fold joints of the Appalachain Plateau, New York and Pennsylvania. *Tectonophysics*, **104**, 299–313.

Bahat, D., Bankwitz, P. and Bankwitz, E., 2003. Preuplift joints in granites: evidence for subcritical and postcritical fracture growth. *Geol. Soc. Am. Bull.*, **115**, 148–165.

Bahat, D., Rabinovitch, A. and Frid, V., 2005. *Tensile Fracturing in Rocks, Tectonofractographic and Electromagnetic Radiation Methods*. Springer-Verlag, Berlin, 569 pp.

Bai, T., Maerten, L., Gross, M.R. and Aydin, A., 2002. Orthogonal cross joints: do they imply a regional stress rotation? *J. Struct. Geol.*, **24**, 77–88.

Bankwitz, P., 1966. Über Klüfte II. Die Bildung der Kluftoberfläche und eine Systematik ihrer Strukturen. *Geologie*, **15**, 896–941.

Bentor, Y.K, Vroman, A. and Zak, A., 1970. *Geological Map of Israel, 1:250,000*. Survey of Israel, Jerusalem.

Cooke, M.L. and Pollard, D.D., 1996. Fracture propagation paths under mixed mode loading within rectangular blocks of polymethyl methacrylate. *J. Geophys. Res.*, **101**, 3387–3400.

De Freminville, M.Ch., 1914. Recherches sur la fragilité –l'éclatement. *Rev. Met.*, **11**, 971–1056.

Flexer, A., 2001. The pre-Neogene geology of the Near East. In: *The Jordan Rift Valley* (A. Horowitz, ed.), pp. 123–171. Lisse, Balkema.

Guin, J.P. and Wiederhorn, S.M., 2003. Crack growth threshold in soda lime silicate glass: role of hold-time. *J. Non-Cryst. Solids*, **316**, 12–20.

Hancock, P.L., Al Kadhi, A., Barka, A.A. and Bevan, T.G., 1987. Aspects of analyzing brittle structures. *Annales Tectonicae*, **1**, 5–19.

Helgeson, D.E. and Aydin, A., 1991. Characteristics of joint propagation across layer interfaces in sedimentary rocks. *J. Struct. Geol.*, **13**, 897–911.

Hodgson, R.A., 1961. Classification of structures on joint surfaces. *Am. J. Sci.*, **259**, 493–502.

Honigstein, A., 1984. Senonian ostracodes from Israel. *Geol. Surv. Isr. Bull.*, **78**, 48.

Jaeger, J.C. and Cook, N.G.W., 1979. *Fundamentals of Rock Mechanics*. Chapman and Hall, New York, 593 pp.

Kerkhof, F., 1975. Bruchmechanische Analyse von Schadensfällen an Gläsern. *Glastech Ber-Glass*, **48**, 112–124.

Krenkel, E., 1924. Der Syrische Bogen. *Centralbl. Mineral. Geol. Palaeontol.*, **9**, 274–281 and **10**, 301–313.

Kulander, B.R., Barton, C.C and Dean, S.C, 1979. *The Application of Fractography to Core and Outcrop Fracture Investigations*. Rep. to U.S.D.O.E. Morgantown Energy Technology Center, METC/SP-79 /3, p. 174.

Lawn, B., 1993 *Fracture of Brittle Solids*.Cambridge University Press, London, 378 pp.

Levi, T., Weinberger, R., Aïfa, T., Eyal, Y. and Marco, S., 2006. Earthquake-induced clastic dikes detected by anisotropy of magnetic susceptibility. *Geology*, **34**, 68–71.

Michalske, T.A., 1977. The stress corrosion limit: its measurement and implications. In: *Fracture Mechanics of Ceramics: Surface Flaws, Statistics, and Microcracking* (R.C. Bradt, A.G. Evans, D.P.H. Hasselman and F.F. Lange, eds), Vol. 5, p. 277. Plenum Press, New York.

Michalske, T.A., 1984. Fractography of slow fracture in glass. In: *Fractography of Ceramic and Metal Failures* (J.J. Mecholsky Jr and S.R. Powell Jr, eds), Vol. 827, pp. 121–136. ASTM STP, Philadelphia.

Mor, U., 1987. *The Geology of the Judean Desert in the Nahal Darga Region*. Israel Geological Survey, Report GSI/21/87, 112 pp. (in Hebrew; English Abstract).

Murgatroyd, J.B., 1942. The significance of surface marks on fractured glass. *J. Soc. Glass Tecl.*, **26**, 155–171.

Parker, J.M., 1942. Regional systematic jointing in slightly deformed sedimentary rocks, *Geol. Soc. Am. Bull.*, **53**, 381–408.

Pollard, D.D. and Aydin, A., 1988. Progress in understanding jointing over the past century. *Geol. Soc. Am. Bull.*, **10**, 1181–1204.

Price, N.J., 1966. *Fault and Joint Development in Brittle and Semi-brittle Rock*. Pergamon Press, New York.

Rawnsley, K.D., Peacock, D.C.P., Rives, T. and Petit, J.P., 1998. Joints in the Mesozoic sediments around the Bristol Channel Basin. *J. Struct. Geol.*, **20**, 1641–1661.

Rives, T., Rawnsley, K.D. and Petit, J.P., 1994. Analogue simulation of natural orthogonal joint set formation in brittle varnish. *J. Struct. Geol.*, **14**, 925–937.

Rubin, A.M., 1995. Propagation of magma-filled cracks. *Annu. Rev. Earth Planet. Sci.*, **23**, 287–336.

Sheldon, P., 1912. Some observations and experiments on joint planes. *J. Geol.*, **20**, 164–183.

Steinitz, G. 1974. *The Deformational Structures in the Senonian Bedded Cherts of Israel*. PhD Thesis, The Hebrew University, 126 pp.

Weinberger, R., 1999. Initiation and growth of cracks during desiccation of stratified muddy sediments. *J. Struct. Geol.*, **21**, 379–386.

Weinberger, R., 2001. Joint nucleation in layered rocks with non-uniform distribution of cavities. *J. Struct. Geol.*, **23**, 1241–1254.

Weinberger, R., Lyakhovsky, V., Baer, G. and Agnon, A., 2000. Damage zones around en echelon dike segments in porous sandstone. *J. Geophys. Res.*, **105**, 3115–3133.

Wiederhorn, S.M., 1967. Influence of water vapor ob crack propagation in soda-lime glass. *J. Am. Ceram. Soc.*, **50**, 407–414.

Wiederhorn, S.M. and Bolz, L.H., 1970. Stress corrosion and static fatigue of glass. *J. Am. Ceram. Soc.*, **53**, 543–548.

Wiederhorn, S.M., Dretzke, A. and Rodel, J., 2002. Crack growth in soda-lime-silicate glass near the static fatigue limit. *J. Am. Ceram. Soc.*, **85**, 2287–2292.

Woodworth, J.B., 1896. On the fracture system of joints, with remarks on certain great fractures. *Boston Soc. Nat. Hist. Proc.*, **27**, 63–184.

Yoda, M., 1990. Subcritical crack growth in soda-lime glass under combined modes I and III loading. *J. Am. Ceram. Soc.*, **73**, 2124–2127.

Received 1 May 2007; revised version accepted 21 November 2007

